J. Hydrol. Hydromech., 71, 2023, 1, 35–48
https://doi.org/10.2478/johh-2022-0040
©2023 Šimon Pospíšilík et al., published by Sciendo. This work is licensed under the Creative Commons Attribution-NonCommercial-NoDerivatives 4.0 International Licence.

sciendo Journal of Hydrology and Hydromechanics Institute of Hydrology SAS

Discharge coefficient, effective head and limit head in the Kindsvater-Shen formula for small discharges measured by thin-plate weirs with a triangular notch

Šimon Pospíšilík*, Zbyněk Zachoval

Brno University of Technology, Faculty of Civil Engineering, Institute of Water Structures, Veveří 331/95, Brno, 602 00, Czech Republic.
* Corresponding author. E-mail: pospisilik.s@fce.vutbr.cz

Abstract: The paper deals with the determination of the discharge coefficient, effective head and newly the limit head in the Kindsvater-Shen formula for the determination of a relatively small discharge of clear water using a thin-plate weir with a triangular notch. The determination of the discharge coefficient, effective head and limit head is based on extensive experimental research and is verified by previous measurements by other authors. The experimental research was characterised by a large range of notch angles (from 5.25° to 91.17°), weir heights (from 0.00 m to 0.20 m), and water temperatures (from 15 °C to 45 °C), as well as a focus on relatively small heads (from 0.02 m to 0.18 m), which is where the strengths of the Kindsvater-Shen formula stand out. The experimental research supplemented existing knowledge about the overflow occurring with small heads and small weir notch angles. The newly determined dependencies in the Kindsvater-Shen formula extended its applicability to weirs with small notch angles and newly enabled the determination of the limit head, which restricts its applicability in the determination of small discharges.

Keywords: Triangular notch (V-notch); Thin-plate weir; Kindsvater-Shen formula; Discharge coefficient; Effective head; Limit head.

INTRODUCTION

Thin-plate weirs (TPWs) used for the determination of water discharge are generally defined by the length of the weir crest in the direction of flow, ranging from 1 mm to 2 mm (ISO 1438, 2017). A triangular notch (also referred as V-notch) is a notch in the wall of a weir which widens in the upwards direction from the bottom of the approach channel. The widening of the notch is usually symmetrical with respect to the longitudinal plane of symmetry of the approach channel. The weir wall is a planar and hydraulically smooth surface with a rectangular upstream weir crest edge. The basic geometric characteristics of a weir located vertically and perpendicularly to the side walls and bottom of an approach channel with a rectangular cross-section comprise the notch angle, the weir height and the distance of the vertical weir axis from the side walls. The overflow is affected by water properties such as viscosity and surface tension. Their values depend mainly on the water temperature and dissolved substances. The overflow is also affected by impurities that adhere to the weir. An important condition for applicability is the requirement for a developed velocity profile in the approach channel.

CURRENT STATE OF KNOWLEDGE

The measurement of water discharge using a TPW with a triangular notch was first proposed by Thomson (1858) for a notch angle of 90°. Subsequently, Thomson (1861) also published the results of follow-up experiments with notch angles of 90° and 126.87°. Barr (1910) undertook the verification and extension of Thomson's (1858, 1861) experiments using other variants of approach channel width and weir height with notch angles of 90° and 54°. Following on from Barr (1910), Strickland (1910) derived a relation for determining the discharge coefficient through experiments. A method of automated water discharge measurement via a TPW with a triangular notch, which involved using a float with an automatic level recorder, was designed by Yarnall (1912). Cozzens (1915) investigated the use and calibration of a TPW with a triangular notch in situ. The effect of water temperature on the coefficient of discharge was investigated by Cozzens (1915) and Switzer (1915). Based on measurements taken, Switzer (1915) evaluated the effect of temperature on the coefficient of discharge as being negligible (up to 2 %) compared to other effects. King (1916) presented a new relationship for calculating the water discharge based on a comparison of his own experimental data with Thomson´s (1858, 1861) and Barr´s (1910) data. Cone (1916) investigated TPWs with rectangular, trapezoidal and triangular notches. Cone subsequently (1917) presented a practical guide for application of TPWs. Barrett (1924) extended the application range to include small heads (> 0.029 m). Mawson (1927) investigated the application of dimensional analysis in Barr´s experimental research (1910). The accuracy of discharge measurement was investigated by Yarnall (1927). O'Brien (1927) presented a mathematical proof that a TPW with a 90° triangular notch offers the highest accuracy compared to other notch angles. Schoder and Turner (1929) investigated the influence of the geometric characteristics of a weir crest on the overflow. Thornton (1929) compared the accuracy of Barr´s (1910) and Yarnall´s (1927) experiments. The effect of viscosity and surface tension on the overflow was investigated by Greve (1930; 1932; 1945) and Lenz (1942). Barrett (1931) and Allerton (1932) investigated the introduction of energy head in the calculation of water discharge. Based on Yarnall´s (1927) research, Smith (1934; 1935) investigated the effect of water temperature. Wirak (1934) published the results of experimental measurements performed on TPWs with a triangular notch. Numachi et al. (1937) investigated the means of attachment of a TPW edge with a triangular notch. Hertzler (1938) investigated the use of TPWs

with a 120° triangular notch in practical applications. Extensive research focusing on the effect of the approach channel width and the weir height for notch angle 90° was conducted by Numachi et al. (1940a; 1940b), Numachi and Hutizawa (1941a; 1941b; 1942a; 1942b). Viparelli (1947) determined the rules for the installation and use of triangular-notch TPWs to measure water discharge. Numachi and Saito (1948; 1951) and also Milburn and Burney (1988) investigated the minimum length of the approach channel and the use of boxes for the placement of TPWs. The measurement of oil discharge overflowing a TPW with a triangular notch was carried out by Itaya and Takenaka (1955). Based on the results of his own experiments and experiments performed by Grossi (1961), Schlag (1962) derived a new relationship for discharge. Shen (1981) summarized the findings of previous experiments on triangular-notch TPWs and he recommended to express the combined effects of surface tension and viscosity of water by defining the effective head and the effective discharge coefficient. Eli (1986) described two methods for the determination of discharge based on measurements of the height and width of the water surface in a notch profile. The collection of water samples using a TPW with a triangular notch was described by Cuttle and Mason (1988). Procedures concerning the selection, installation and use of TPWs to measure discharge were published by Bos (1989). Ghodsian (2004) obtained a new relationship for the calculation of coefficient of discharge. Martínez et al. (2005), Piratheepan et al. (2007) and Ali et al. (2015) investigated composite TPWs with a triangular notch. Ji (2007) and Ramamurthy et al. (2013) experimentally investigated TPWs with several triangular notches. A comparison of TPWs with rectangular, trapezoidal and triangular notches, supplemented with measurement error determination, was performed by Martikno et al. (2013). Chanson and Wang (2012; 2013) investigated the calibration of TPWs with a triangular notch under unsteady flow. Bautista-Capetillo et al. (2013) investigated the use of slow-motion photography to determine the discharge coefficient. Caroline and Afshar (2014) published the effect of the bed slope of the approach channel on the overflow. A comparison of flow through TPWs with rectangular and triangular notches was carried out by Adeyemi et al. (2017). Reddy and Reddy (2017) presented the results of research concerning the effect of water density (clear and muddy) on the discharge coefficient. Hattab et al. (2019) investigated the use of gauging TPWs with a triangular notch in confined conditions (2019). Vatankhah and Khamisabadi (2019) investigated the shape of the triangular notch and notches with curved extensions. Experiments with a 2.67° notch angle were carried out by Pospíšilík (2020). Vicena (2020) determined the minimum overflow height depending on the triangular notch angle of a TPW. Pospíšilík (2021) investigated the identification and quantification of uncertainties in determining the coefficient of discharge. Pospíšilík (2022) analysed the extent to which overflow through TPWs with a triangular notch has been explored.

The above overview demonstrates that research in the field of TPWs with a triangular notch has been taking place intensively for a great many years, and that it is far from complete. Basic research associated with TPWs with a triangular notch has a direct impact on their applicability in practice. Triangular notch TPW are widely used for the determination of discharge, and this led to their inclusion in the ISO 1438 (2017) standard.

THEORY

The equations for determining the discharge Q overflowing a TPW with a triangular notch can be divided according to the method of derivation into analytically derived, semi-empirical and empirical. For analytical derivation the energy conservation equation or the momentum equation (submerged weirs) are used, for semi-empirical method dimensional analysis is used in addition to the above. According to the method of calculation, the equations can be divided into implicitly or explicitly expressed. As far as practical use is concerned, explicitly expressed relations where the discharge is calculated directly on the basis of measured quantities are more commonly employed.

The measured quantities at a free overflow are the notch angle α, the approach channel width B, the level of the approach channel bottom Z_b, the level of the weir crest Z_P, and the water surface level Z_h at an agreed distance upstream from the weir ($2h_{max}$ to $4h_{max}$, where h_{max} is the maximum head (ISO 1438, 2017)). From the values of the levels, the weir height is calculated $P = Z_P - Z_b$, as well as the head $h = Z_h - Z_P$.

Worldwide, the most widely used equation for the determination of water discharge using a TPW with a triangular notch is currently the Kindsvater-Shen (Shen, 1981)

$$Q_C = C_d \cdot \frac{8}{15} \cdot \tan\frac{\alpha}{2} \cdot (2 \cdot g)^{1/2} \cdot h_e^{5/2}, \tag{1}$$

which is explicitly expressed semi-empirical equation based on the energy conservation equation and the experimental measurements, where C_d is the discharge coefficient, g is acceleration due to gravity (9.80665 m·s^{-2}) and h_e is the effective head. Effective head

$$h_e = h + k_h \tag{2}$$

expresses, using the height

$$k_h = f_1\{\alpha\} \tag{3}$$

the combined effect of the viscosity and surface tension of clear water. It is assumed that the effect of the change in water temperature T in the range of 5 °C to 30 °C (Bos, 1989) (causing the change in density, viscosity and surface tension of water) is negligible. The applicability of the calculation method for precise flow discharge measurement is limited by Shen (1981) to a minimum head of h_s = 0.06 m, a minimum notch angle of 20° and a maximum notch angle of 100°, at which, according to Shen (1981), instabilities of the nappe begin to appear, or there is a lack of measured data. Due to the inconsistencies in the measured data, the calculation method is also limited to a minimum weir height of 0.09 m.

Based on the evaluation of data from the measurements of the above-mentioned authors as well as our own data it was found that the lower limit h and α of the applicability of the Kindsvater-Shen method of calculation is not so much due to the instability of the nappe, but primarily to the change in the dependence of C_d on h. For this reason, the calculation method newly incorporates limit head h_l, which defines the lower limit of the application area of the modified calculation method. Thus, for values $h \geq h_l$, where

$$h_l = f_2\{\alpha\}, \tag{4}$$

it is possible to use the Kindsvater-Shen calculation method, otherwise not.

The coefficient C_d is a function of only three variables when function (3) is valid (Shen, 1981) and when the limiting condition $h \geq h_l$ stated above is fulfilled

$$C_d = f_3\left\{\frac{h}{P}, \frac{P}{B}, \alpha\right\}. \tag{5}$$

Assuming a sufficiently large value of B (or small P/B ratio), independence from P (or h/P) can be expected, which in the new defined range $h \geq h_l$ leads to the simplification of the functional dependence (5) on

$$C_d = f_4\{\alpha\}. \quad (6)$$

It is possible to determine the functional dependencies (3), (4) and (5) (or (6)) on the basis of experimental measurements. Although a considerable number of measurements have been made, there is still a lack of data in the region of small values of h and α (Pospíšilík, 2022; Shen, 1981), so extensive experimental research has been carried out in Brno University of Technology (BUT).

EXPERIMENT

A short rectangular flume (box) with a length 1.23 m, width B = 0.50 m and height 0.43 m (Fig. 1) was used. The flume was made of waterproof plywood with a smooth finish. At the end of the flume, there was a frame structure to which the investigated TPWs with a triangular notch (angles α = 5.25°; 10.18°; 15.19°; 20.23°; 25.21°; 30.53°; 60.67° and 91.17°) were inserted. The value α was determined by the two-cylinder method (ISO 1438, 2017; Pospíšilík, 2020). The frame structure prevented the deflection of the weir plate, allowed the centring of the weir in the flume and enabled vertical changes to be made to the position of the weir plate. By vertically changing the position of the weir plate, the selected value P was set at five height levels (Table 1). The TPWs were made from 1 mm thick stainless-steel sheeting, the notch edges were right-angled. In the flume, at a distance of 0.82 m from the weir, a flow straightener was placed to ensure the uniform distribution of longitudinal velocities along the cross-section profile of the flume (Fig. 2, white plates). The flow straightener consisted of two pairs of perforated plates with circular holes of 38 mm diameters spaced 20 mm apart. The distance between each pair of plates was 0.20 m. The paired arrangement of the plates enabled the size of the openings in the regulating element to be changed via the vertical displacement of one plate of the respective pair. In order to limit the formation of waves on the water surface, a floating plate made of expanded polystyrene with a width 0.49 m, length 0.25 m and thickness 0.015 m was placed downstream of the regulating element. The mentioned elements ensured the even distribution of longitudinal velocities in the cross-section profile with the measurement of the water surface level, which was confirmed by measuring the field of longitudinal velocities (Pospíšilík et al., 2022). The flume was connected to a hydraulic system with water recirculation. The water was supplied by a hose to the damping part of the flume and flow freely over the TPW into a storage tank. The discharge was provided by two pumps; it was possible to define the frequency of revolutions of the pump to set the desired value of Q. To quantify the effect of a change in water temperature T, which causes a change in viscosity and surface tension, a pair of 2 × 1000 W heaters was placed in the storage tank.

The value of Q was determined using the volume method ($Q \leq 0.00003$ m^3·s^{-1}, expanded combined uncertainty up to 0.52 %, graduated cylinders of class A), the mass method ($Q \leq 0.00050$ m^3·s^{-1}, expanded combined uncertainty up to 0.42 %, calibrated scales), and also calibrated electromagnetic flowmeters (expanded combined uncertainty 2 %) with the diameters DN10 (0.000016 m^3·s^{-1} ≤ Q ≤ 0.00050 m^3·s^{-1}) and DN32 (0.00033 m^3·s^{-1} ≤ Q ≤ 0.0034 m^3·s^{-1}). The time for determining the discharge was at least 180 s. Measurement of the Z_b, the upper surfaces of the inserted cylinders and the Z_h was carried out using a digital point gauge with a resolution of 0.01 mm placed on a cross beam in the longitudinal plane of symmetry of the flume. The Z_h for the determination of h was measured at a distance of 0.38 m upstream from the weir plate ($2h_{max}$). The B was measured using a calibrated metal tape gauge with a resolution of 1 mm. The T was measured with a digital thermometer with a resolution of 0.1 °C.

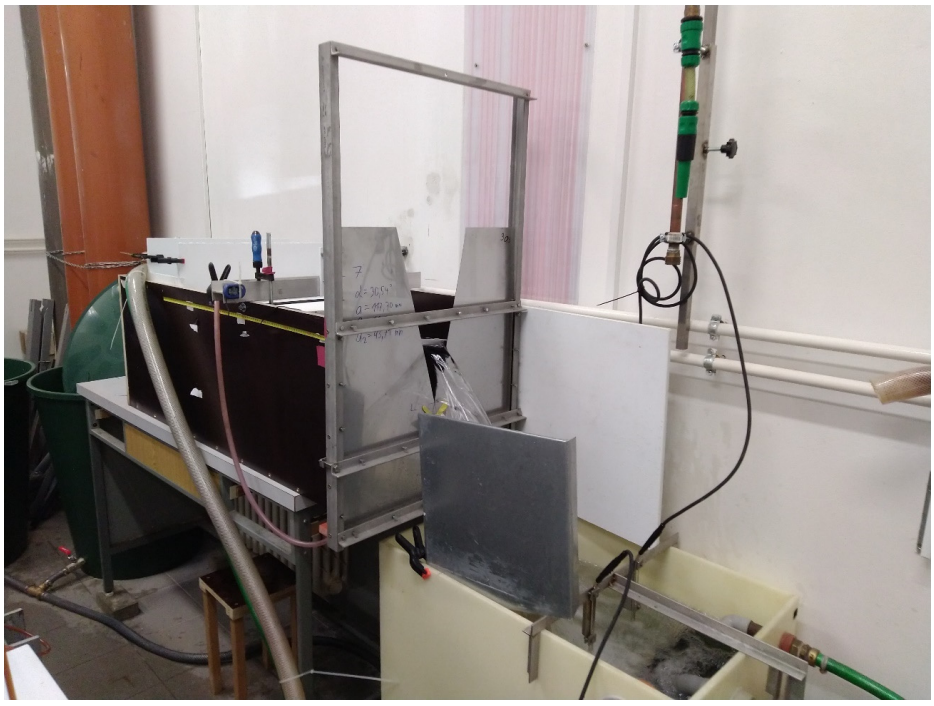

Fig. 1. Experimental equipment.

Table 1. Ranges of the measured quantities.

α [°]	P [mm]	h [mm]	T [°C]	$Q \times 10^{-3}$ [m^3·s^{-1}]
05.25	0.53; 49.51; 100.65; 100.71; 150.65; 198.85	51.07–181.31	15.1–19.5	0.0425–1.0089
	1.98; 50.81; 99.18; 100.65; 150.05; 198.75	29.32–180.46	38.4–42.5	0.0090–1.0128
10.18	0.86; 50.38; 98.60; 99.97; 151.06; 200.34	44.46–180.68	16.0–18.3	0.0589–1.8917
	0.68; 50.05; 98.60; 99.15; 151.94; 199.30	30.13–180.79	38.8–43.4	0.0209–1.9011
15.19	0.10; 50.51; 98.61; 100.54; 149.38; 200.33	48.59–181.12	16.0–18.5	0.1087–2.7722
	1.78; 50.85; 98.61; 100.30; 148.79; 196.96	30.45–181.38	39.0–45.0	0.0327–2.7722
20.23	0.46; 50.16; 98.61, 100.26; 150.86; 201.12	46.84–180.76	15.8–19.2	0.1320–3.6116
	1.76; 50.00; 98.61; 98.70; 150.00; 197.70	29.81–180.52	39.1–45.3	0.0408–3.6461
25.21	0.89; 50.60; 96.58; 101.46; 150.49; 200.87	45.39–167.53	14.7–19.5	0.1517–3.6588
	0.52; 51.16; 96.58; 100.44; 149.22; 199.62	29.31–166.67	39.0–44.1	0.4888–3.6950
30.53	0.57; 50.90; 98.83; 99.85; 149.35; 200.60	45.66–155.27	16.2–19.7	0.1857–3.6627
	0.85; 51.17; 98.83; 101.42; 151.47; 200.58	19.81–154.56	36.2–42.3	0.0233–3.6661
60.67	0.23; 49.58; 97.59; 99.75; 150.10; 199.93	40.41–115.48	14.5–19.5	0.2677–3.6577
	1.32; 51.10; 97.59; 101.97; 152.32; 201.36	20.24–114.72	39.0–43.4	0.0472–3.6816
91.17	0.46; 50.23; 99.43; 102.70; 149.80; 199.82	39.33–93.26	15.9–18.1	0.4188–3.6522
	0.31; 50.34; 100.87; 102.70; 150.65; 199.07	20.19–93.47	39.1–44.0	0.0744–3.6994

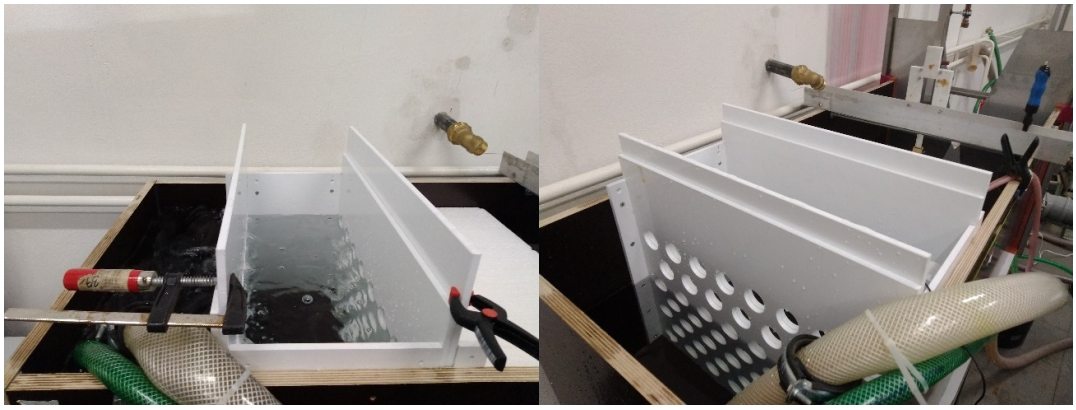

Fig. 2. Flow straightener.

The measurement of all the above quantities was always carried out under a steady state of flow. The range of Z_h measurements was limited by the maximum head $h_{max} = 0.18$ m and the head when the nappe adheres to the downstream face of weir plate (which depends on the α value). To verify the effect of the T on the Q, measurements were made in two ranges of T values. The first range was from 15 °C to 20 °C, while the second was from 36 °C to 45 °C. The range of the measured data is shown in Table 1. A detailed description of the experimental equipment, gauges and measurements was published by Pospíšilík (2020). Uncertainties affecting C_d were identified and quantified (Pospíšilík, 2021) according to the Guide to the Expression of Uncertainty in Measurement (JCGM 100, 2008).

DATA PROCESSING METHOD AND ITS EVALUATION

The data processing method consisted in finding such values of C_d, k_h and h_l that C_d is constant for a relevant α in the range $h_l \le h \le h_{max}$. This was achieved in such a way that from $h = 0.015$ m the h was divided into intervals per $\Delta h = 0.010$ m (interval Δh_1 is from $h = 0.015$ m to $h = 0.025$ m, interval Δh_2 is from $h = 0.025$ m to $h = 0.035$ m, etc.). Separately for given α and for given interval the average value of the discharge coefficient $\bar{C}_d$ was calculated from all the measured values C_d in that interval (for given α in the interval Δh_1 are values $C_{d1,1}$, $C_{d1,2}$, etc. for which the average value $\bar{C}_{d1}$ was calculated; for interval Δh_2 are values $C_{d2,1}$, $C_{d2,2}$, etc. for which the average value $\bar{C}_{d2}$ was calculated; etc.). A linear function with zero direction was drawn through the values $\bar{C}_d$. The value h_l and simultaneously the value k_h were sought in order to achieve a constant $\bar{C}_d$ in the largest possible range of h (iterative process). The invariance of $\bar{C}_d$ on h was evaluated by an approximation line segment with a zero direction in the range $h_l \le h \le h_{max}$. The value h_l was determined by a deviation of ±1 % from the average of $\bar{C}_d$ values determined in the range $h_l \le h \le h_{max}$.

For a detailed illustration of the above-mentioned method and its evaluation, the dependencies of C_d, k_h and h_l on h are shown in the graphs. Fig. 3 shows the dependence of C_d on h for individual α. They are supplemented with values for $\bar{C}_d$, and the course of the linear approximation curve with a zero direction and a deviation of ±1 %. The values of the approximation curve correspond to the value C_d of approximation curve (7). The graphs in Fig. 3 are supplemented by the definition of value h_l determined by relation (9). A division in the dependence of C_d at h_l is evident. The dependence of C_d on h can be considered linear (invariant) for the area $h_l \le h \le h_{max}$. For the values $h < h_l$, the linear dependence does not apply, and the C_d values decrease.

6 types of regression functions were used for the determination of functional dependencies (3), (4) and (6). The appropriateness of the chosen regression function was assessed by comparing the values of the coefficients of determination R^2.

In order to demonstrate the invariance of k_h on h in the range $h_l \le h \le h_{max}$, the graphs in Fig. 4 show the dependence of k_h on h for individual values of α. They are supplemented with the course of the linear approximation curve with a zero direction

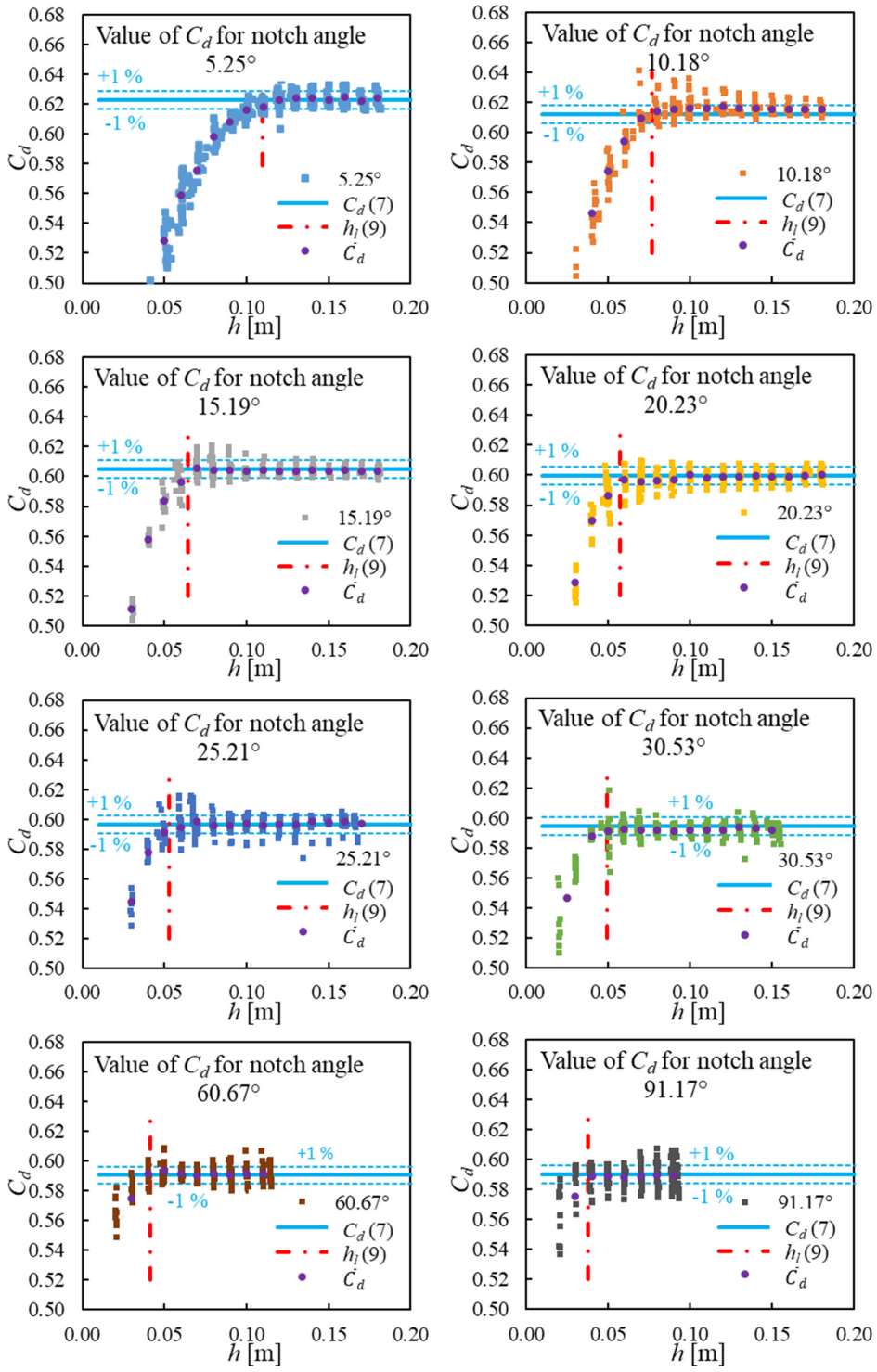

Fig. 3. Evaluation of the dependence of C_d on h for individual values of α; determination of h_l.

and a deviation of ±1 mm. The values of the linear approximation curve correspond to the value k_h of approximation curve (8). Also here, a division in the dependence of k_h is visible at the location of the h_l value. The dependence of k_h on h can be considered linear (invariant) for the area $h_l \le h \le h_{max}$. For values $h < h_l$, the linear dependence does not apply and the k_h values decrease. The values k_h in the range $h_l \le h \le h_{max}$ lie, with some exceptions, within the limits of a deviation of ±1 mm from the approximation curve. For a comprehensive verification of the correctness of the method used, a correlation matrix was created between C_d and the variables of function (5) in the range $h_l \le h \le h_{max}$. The correlation matrix shows a significant dependence only between C_d and α. The dependence of C_d on the ratios P/B and h/P is negligible.

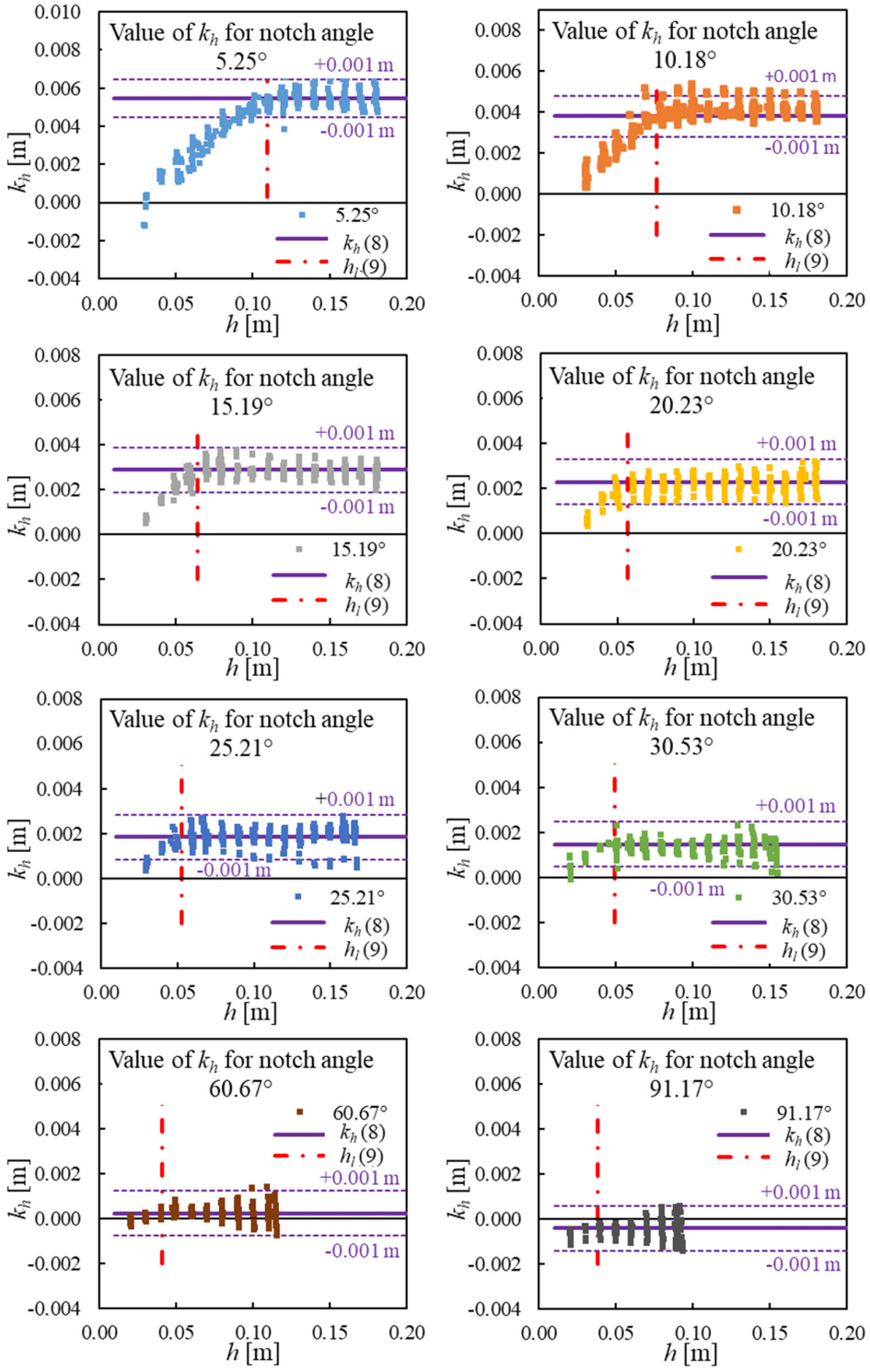

Fig. 4. Evaluation of the dependence of k_h on h.

RESULTS AND DISCUSSION

The main result is the quantification of functional dependencies (3), (4) and (6) by the above-mentioned method using the measured data in the range $h_l \leq h \leq h_{max}$. For $\alpha = 91.17°$, it is valid only for $P/B \leq 0.2$. The parameters in the equations were rounded to the minimum number of significant digits in such a way that the rounding has no effect on the calculated value with three significant digits.

The dependence of C_d on α (6) was described by an approximation curve

$$C_d = 0.05 \cdot \exp(-0.08 \cdot \alpha) + 0.59 \quad (7)$$

with $R^2 = 0.983$. The approximation curve, together with the values C_d determined from the measurements for the individual values α and k_h calculated according to Equation (8), is shown graphically in Fig. 5 and supplemented with a deviation of ±1 %.

For comparison, the dependence is supplemented with a Shen curve (1981). The area delimited by the ±1 % deviation of the approximation curve contains a significant part of the measured values C_d. Compared to the curve presented by Shen (1981), the approximation curve shows higher C_d values across the entire range of values and has a different shape of dependence.

The dependence of k_h on α (3) was described by an approximation curve

$$k_h = 0.0194 \cdot \alpha^{-0.186} - 0.0088 \quad (8)$$

with $R^2 = 0.997$. The dependence is shown together with the values determined from the measurements and a deviation of ±0.001 m in the graph in Fig. 6. The graph is supplemented by a curve presented by Shen (1981). The approximation curve describes the values k_h in the whole range of measured values α. Compared to the curve defined by Shen (1981), the approximation curve shows lower k_h values across the entire range of α.

The dependence of h_l on α (4) was described by an approximation curve

$$h_l = 0.3 \cdot \alpha^{-0.8} + 0.03 \quad (9)$$

with $R^2 = 0.945$. The approximation curve supplemented with the h_l values determined in the aforementioned way is shown in the graph in Fig. 7. Fig. 7 is supplemented with the boundary area of the measured data and the curve h_s stipulated by Shen (1981), who determined it mainly because of the instability of the nappe and the lack of measured data. It can be seen from the graph that the approximation curve of h_l aptly intersects the values determined by the above-mentioned method of evaluation. In the range of intersection of the values α determined by Shen (1981) and the measured values (10° to 90°), the approximation curve shows a different course of values h_l compared to the values h_s presented by Shen (1981). In the area of $h_l \leq h \leq h_{max}$, the instabilities of the nappe mentioned by Shen (1981) were not observed. The lower value of h_l in the area of 20° to 90° quite significantly expands the application area of the use of TPWs with a triangular notch for the determination of small values of Q. In the range of values α from 10° to 20°, on the other hand, the application range is reduced, and in the range of α from 5° to 10° it is newly determined.

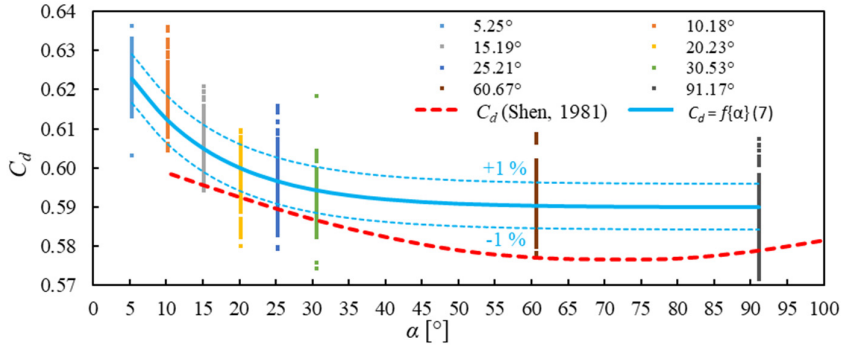

Fig. 5. Dependence of C_d on α.

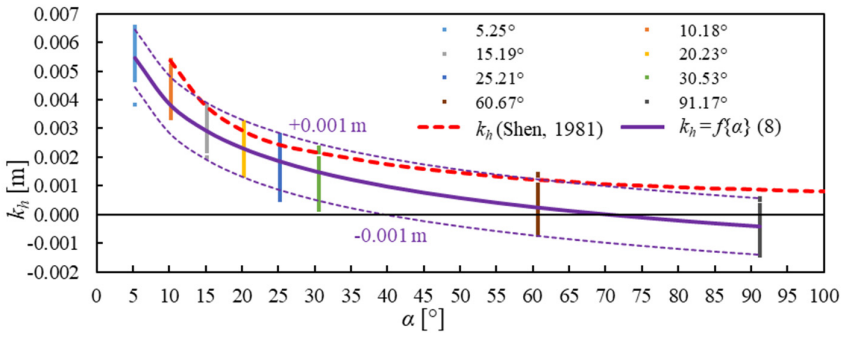

Fig. 6. Dependence of k_h on α.

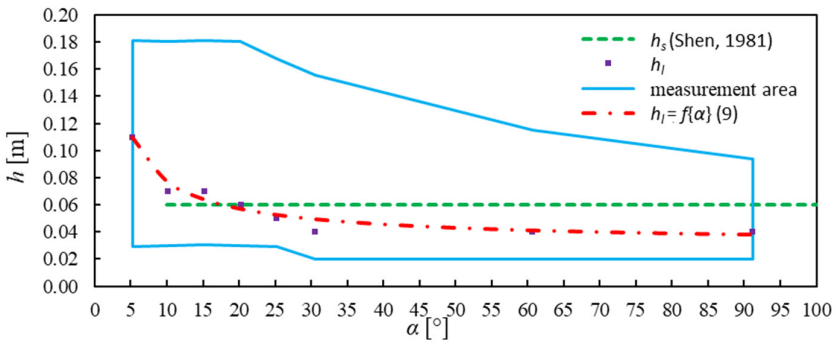

Fig. 7. Dependence of h on α.

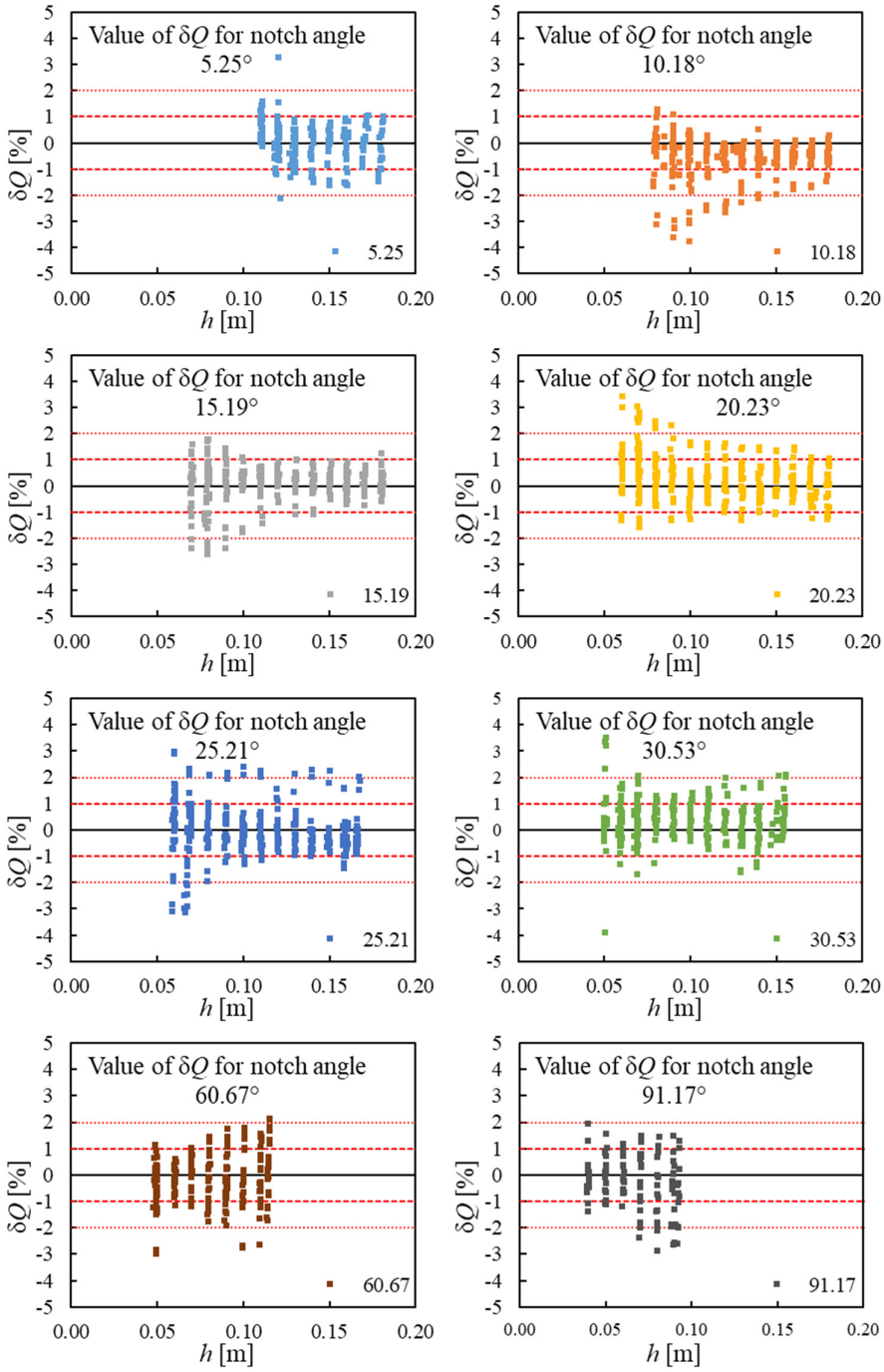

Fig. 8. Evaluation of the dependence of δQ on h for individual α.

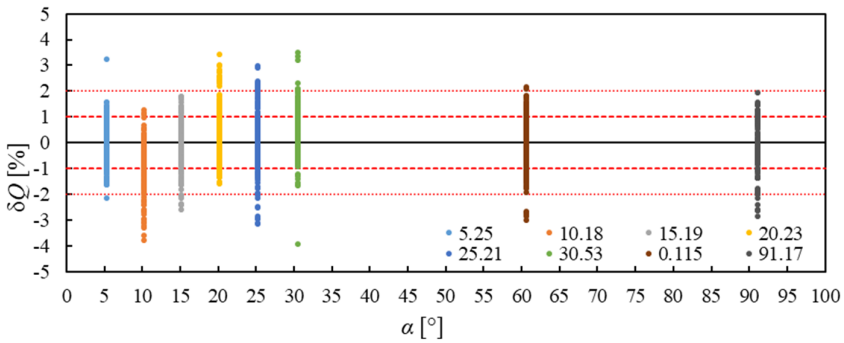

Fig. 9. Dependence of δQ on α.

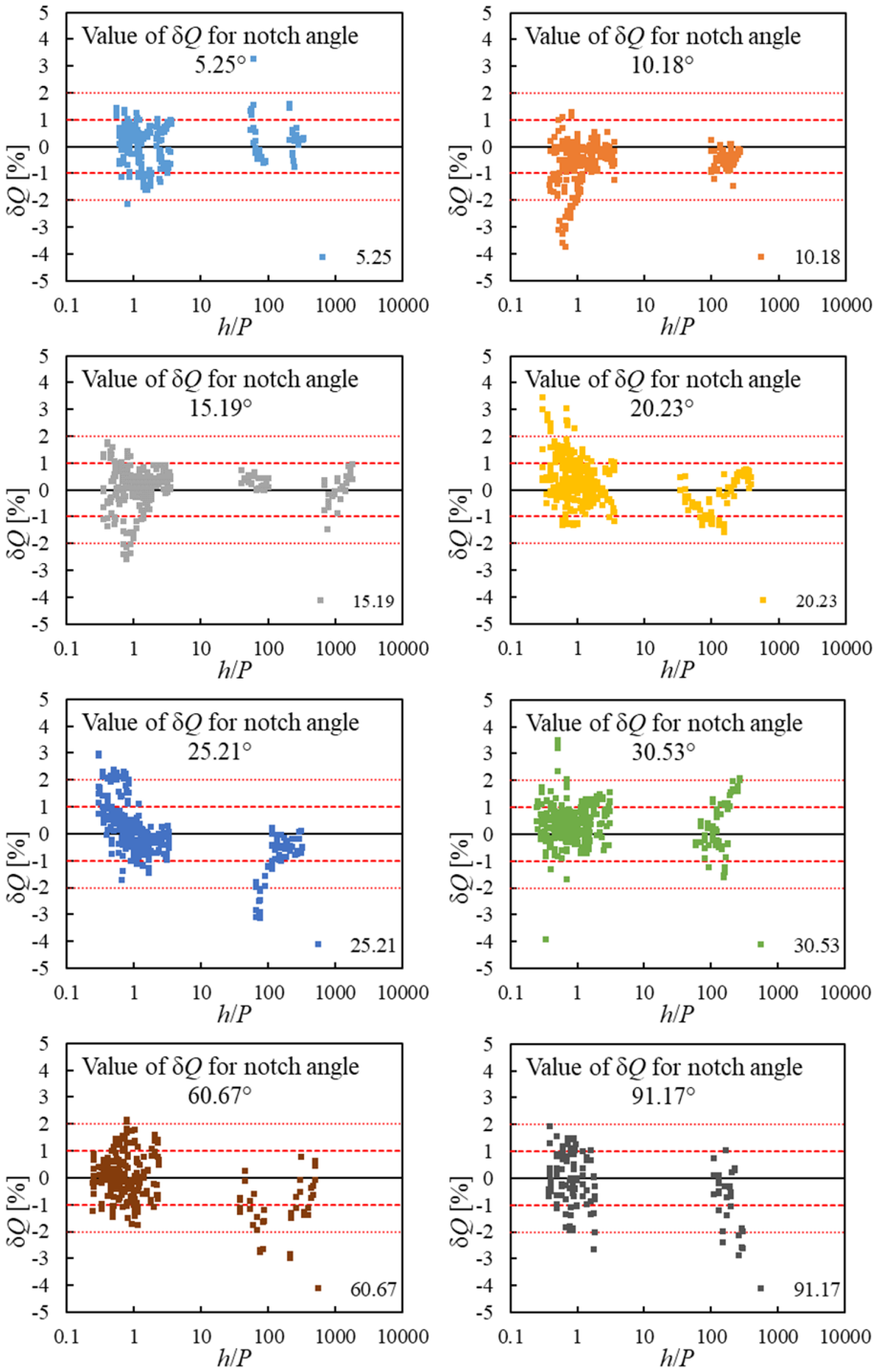

Fig. 10. Evaluation of the dependence of δQ on the ratio h/P.

Equations (7), (8) and (9) quantify the functional dependencies (3), (4) and (6). In this way, the values of Q can be calculated in the validity ranges of $5° \leq \alpha \leq 90°$, $0.00\ \text{m} \leq P \leq 0.20\ \text{m}$ and $h_l \leq h \leq h_{max}$ with h_{max} defined by the extent of the area depicted in the graph in Fig. 7. The validity of the equations for $\alpha = 91.17°$ is also limited by the ratio $P/B \leq 0.2$, which, to some extent, confirms the conclusions of Numachi and Hutizawa (1941a; 1941b). Application for $h > h_{max}$ (extrapolation) is not possible, because the overflow is affected by scale effect and missing measured data for majority of notch angles. The validity of the equations is further limited by the characteristics of the flume (box). The advantages of the aforementioned method for the determination of Q are, unlike in the case of other methods recommended by various authors, the large application range for determining small values of Q, the comprehensive option for calculation without the need to use graphs (ISO 1438, 2017), the relative simplicity of the dependencies (functional dependencies are expressed only by α), and the accuracy of the determination.

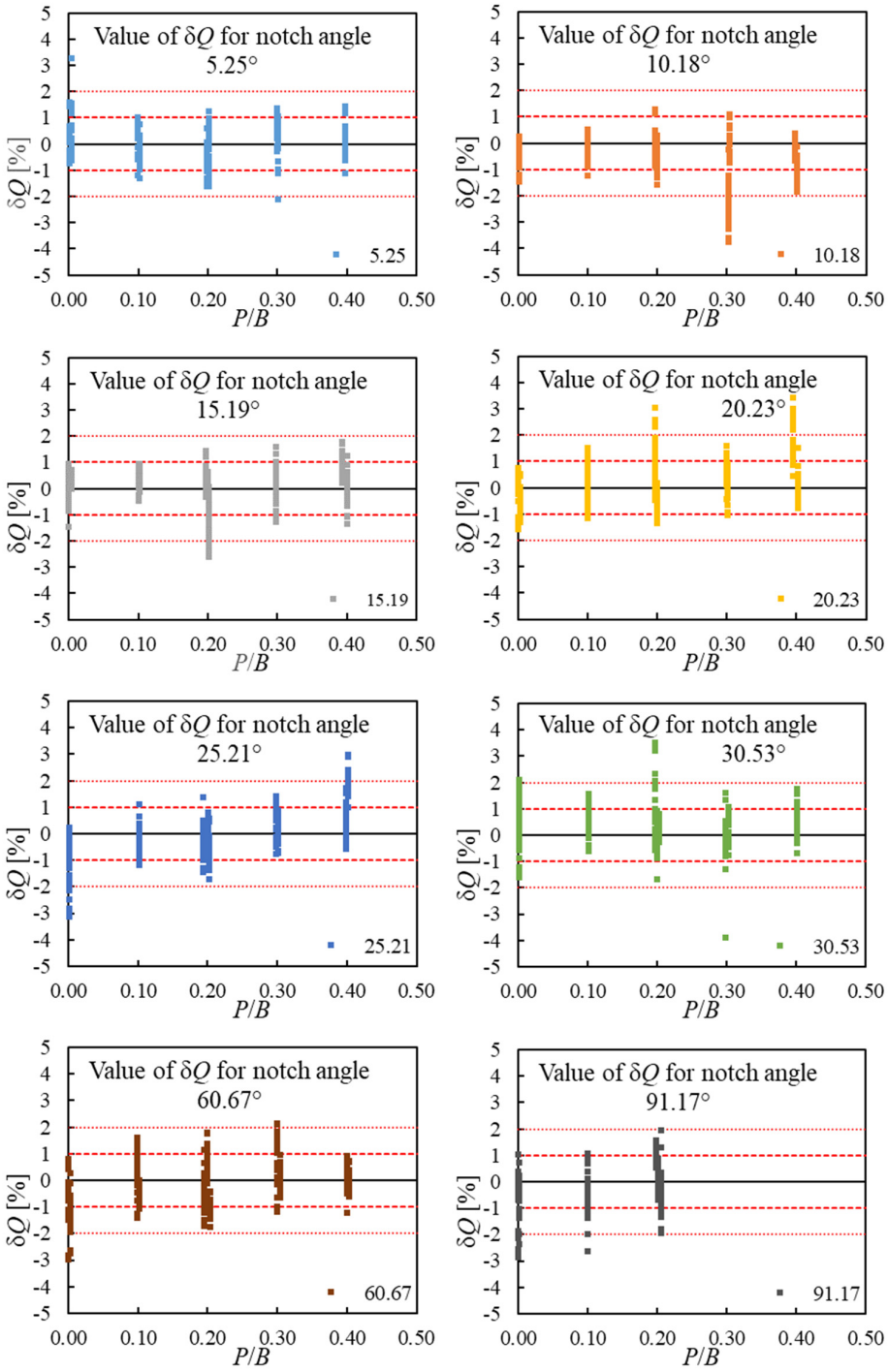

Fig. 11. Evaluation of the dependence of δQ on the P/B ratio.

A detailed analysis of the accuracy of the discharge determination using relationships (1), (2), (7), (8) and (9) can be performed by comparing the calculated discharge Q_C and the measured discharge Q using the relative error

$$\delta Q = \frac{Q_C - Q}{Q}. \tag{10}$$

Two functional dependencies are stated. The dependence of δQ on h for all values of α is shown in the graph in Fig. 8. The dependence of δQ on α is shown in the graph in Fig. 9. The distribution of δQ values in the interval ±1 % can be considered invariant with regard to h with some exceptions (Fig. 8). The vast majority of values for both dependencies lie within the interval ±1 %. The values outside the interval ±2 % are likely to originate from measurement inaccuracies.

A detailed evaluation of the validity of the simplification of functional dependence (5) on dependence (6) in the range $h_l \leq h \leq h_{max}$ and for $\alpha = 91.17°$ also in the range $P/B \leq 0.2$, i.e.

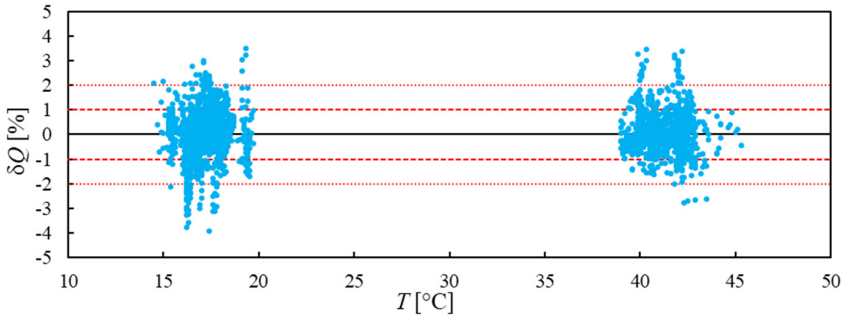

Fig. 12. Dependence of δQ on T.

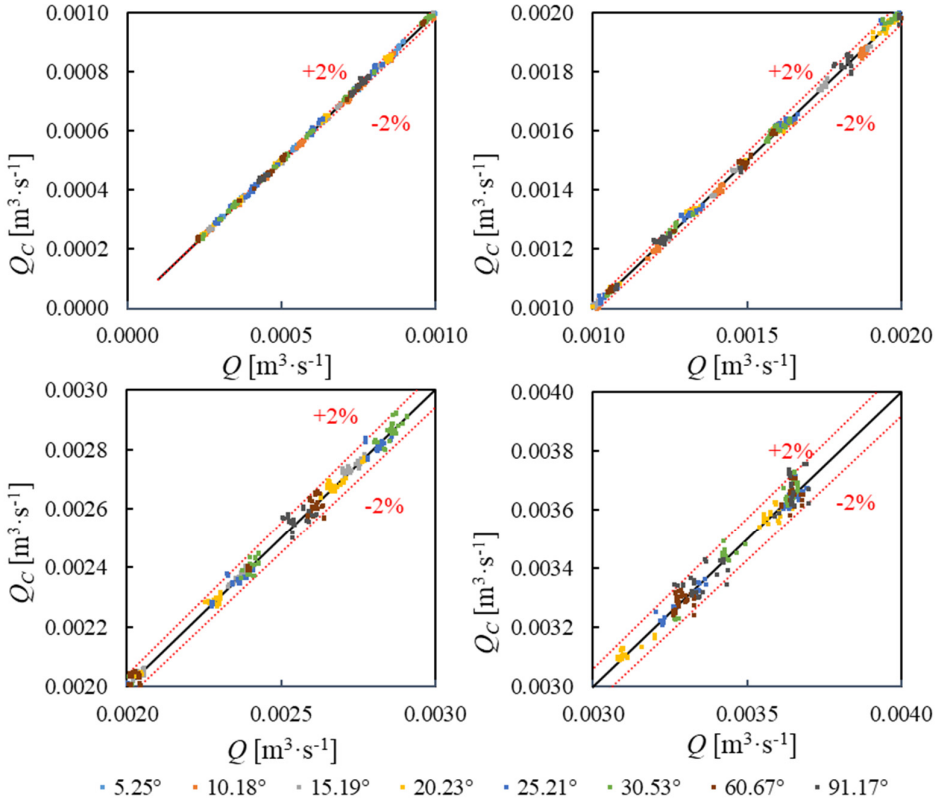

Fig. 13. Comparison of Q_C and Q.

the influence of ratios h/P and P/B on δQ, is shown graphically in Fig. 10 and Fig. 11 for individual values of α. No dependence is obvious from the distribution of values δQ on h/P or on P/B. The vast majority of δQ values lie within the interval ±1 %. The values outside the interval ±2 % are likely to originate from measurement inaccuracies. The graphs in Fig. 10 and Fig. 11 confirm the independence of δQ from the ratios h/P and P/B in the range $h_l \leq h \leq h_{max}$.

Confirmation of the validity of neglecting the effect of the water temperature change in the total range of 15 °C ≤ T ≤ 45 °C for $h_l \leq h \leq h_{max}$ for the above-mentioned evaluation method is shown graphically in Fig. 12. The graph shows the dependence of δQ on T and proves that the effect of the temperature change in the range $h_l \leq h \leq h_{max}$ is too minor to calculate within the framework of the uncertainties when determining Q.

A direct comparison of values Q_C and Q is shown in the graph in Fig. 13. The graph is supplemented with a line of agreement for their values. The Q_C values follow the line of agreement and confirm the suitability of the relations used over the entire range of the Q values measured. The histogram of δQ was performed which showed that 79.1 % of the values are within the ±1 % interval and 95.5 % of the values are within the ±2 % interval.

Verification of the accuracy of the calculation method is carried out by comparing the values Q_C and measured values of Q from selected authors in Fig. 14. The majority of the Q_C values lie near the line of agreement. With some exceptions, the Q_C values up to the $Q = 0.0017$ m^3·s^{-1} are very close to the line of agreement but above the mentioned value, some of them deviate. The deviation maintains the same trend. The effect of the deviation is probably caused by the different characteristics of the approach channel and the accuracies of the experimental measurements of the individual authors. Fig. 14 shows the relatively large deviation of Barrett´s (1924) values from the values of other authors. The deviation of Barrett's (1924) values may be caused for big values of discharges by the use of a short measurement time interval (10 s) and for small values of discharges by the clinging of water to the weir plate.

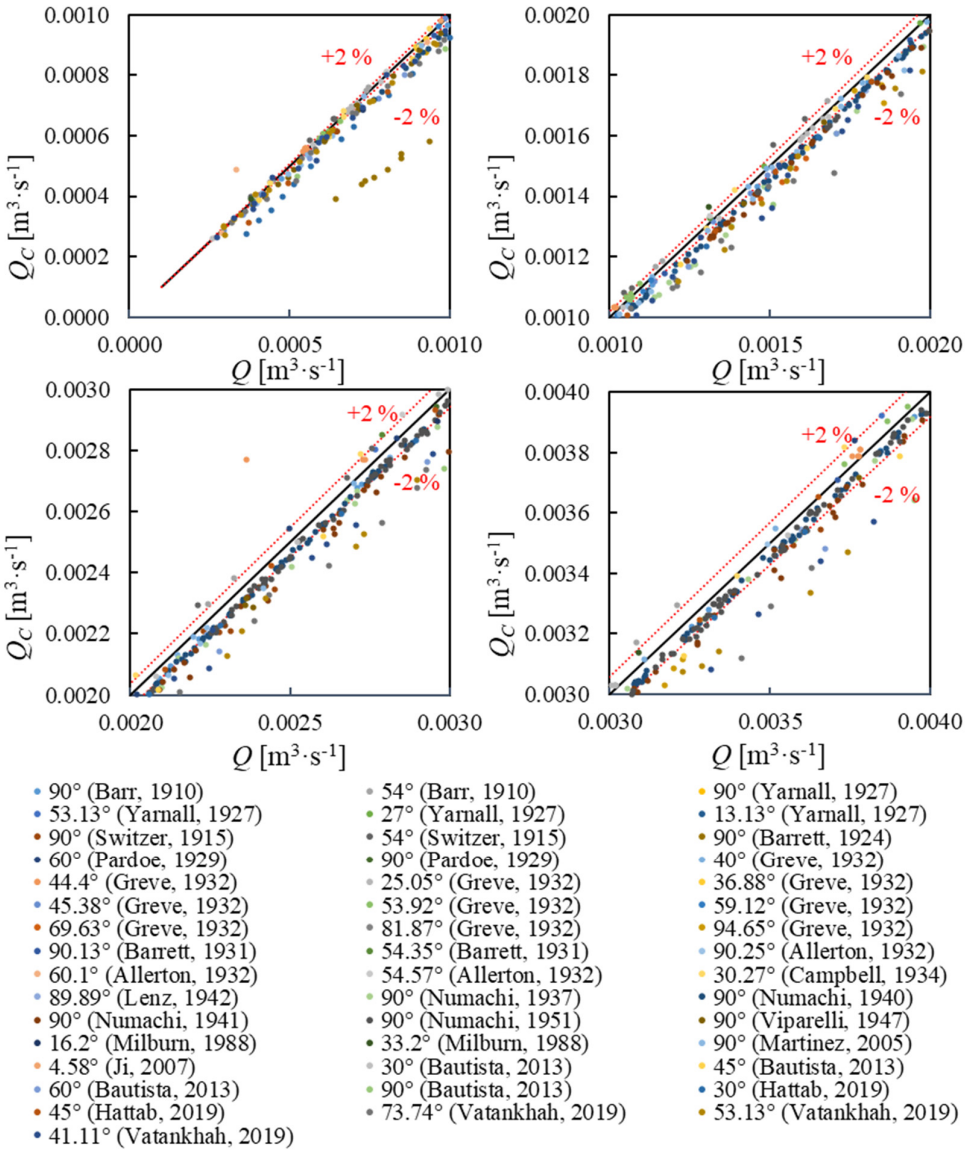

Fig. 14. Comparison of Q_C values and the Q values of other authors.

CONCLUSION

The application range of the calculation method according to Kindsvater-Shen (Shen, 1981) for the determination of Q using a TPW with a triangular notch is relatively limited for the determination of small values of Q, which is due, among other things, to the instability of the nappe and the amount of measured data. Due to a lack of measured data, extensive experimental research was carried out in which it was possible to take measurements in the range of $5.25° \leq \alpha \leq 91.17°$, $0.00\ \text{m} \leq P \leq 0.20\ \text{m}$, $0.020\ \text{m} \leq h \leq 0.18\ \text{m}$ and $15\ °\text{C} \leq T \leq 45\ °\text{C}$. The evaluation of the experimental measurements included the determination of their uncertainties. The results from the experimental measurements formed the basis for extending the applicability and modification of the Kindsvater-Shen method of calculation.

The Kindsvater-Shen method of calculation does not take into account h_l, which limits from below the area of applicability of the invariant dependence of C_d on h at the relevant α. Only the value h_s is given due to nappe instability and the limited amount of measured data. Due to the limitations of the applicability of the Kindsvater-Shen calculation method, h_l was newly incorporated, and its dependence on α was determined. The modified method of calculation of Q consisted in finding such values of C_d, k_h and h_l that C_d is invariant for the respective α in the range $h_l \leq h \leq h_{max}$. The modified method of calculation (compared to the original method) significantly expands the application area and defines it from below, mainly with regard to the determination of small values of Q.

The independence of the modified method of calculating Q from ratios h/P, P/B, and also from T in the entire range of values $h_l \leq h \leq h_{max}$ and the range of values α, P, B and T was proved. The exception was a TPW with $\alpha = 91.17°$, for which independence is valid only for $P/B \leq 0.2$, which to some extent confirms the conclusions of Numachi and Hutizawa (1941a; 1941b).

A detailed analysis of the accuracy of the determination of Q in relation to both h and α for $h_l \leq h \leq h_{max}$ was conducted. It was evaluated using δQ. The majority of the δQ values were within the ±1 % interval, and the vast majority of the δQ values were within ±2 %.

A results from frequency histogram of δQ was also presented. It confirmed the high accuracy of determination using the newly adapted calculation method. To verify the applicability of the adapted calculation method in the whole range of the measured values Q, calculated values Q_C were compared with experimentally measured. The correctness of the adjusted calculation method was thus confirmed across the entire range of measured values of Q.

Verification of the accuracy of the adjusted calculation method was performed by comparing the values of Q_C and the values of Q measured by all the authors mentioned above. The agreement in the area of determining small discharges is obvious.

Acknowledgements. The contribution was created with the support of project FAST-J-21-732 "Flow over thin-plate weirs with triangular notches with small heads".

REFERENCES

Adeyemi, O.I., Oreko, B.U., Abam, J., 2017. Experimental determination of the effect of notch shape on weir flow characteristics using constant head discharge apparatus. Asian J. Curr. Res., 2, 2, 55–64.

Ali, A.A.M, Ibrahim, M., Diwedar, A.I., 2015. The discharge coefficient for a compound sharp crested V-notch weir. Asian J. Eng. Technol., 3, 5, 494–501.

Allerton, R.W., 1932. Flow of water over triangular weirs. Thesis. Princeton University, Princeton.

Barr, J., 1910. Experiments upon the flow of water over triangular notches. Engineering, 89, 435–437, 470–473.

Barrett, F.B., 1931. The flow of water over triangular weirs. Thesis. Princeton University, Princeton.

Barrett, J.M., 1924. A study of the flow of water over triangular weirs and the determination of coefficients of discharge for small heads. Thesis. Utah Agricultural College, Logan.

Bautista-Capetillo, C., Robles, O., Júnez-Ferreira, H., Playán, E., 2013. Discharge coefficient analysis for triangular sharp-crested weirs using low-speed photographic technique. J. Irrig. Drain. Eng. - ASCE, 140, 3, 06013005.

Bos, M.G., 1989. Discharge measurement structures. 3. ILRI.

Caroline, L.L., Afshar, N.R., 2014. Effect of types of weir on discharge. J. Civ. Eng. Sci. Technol., 5, 2, 35–40. https://doi.org/10.33736/jcest.137.2014

Cone, V.M., 1916. Flow through weir notches with thin edges and full contractions. J. Agric. Res., 5, 23, 1051–1113.

Cone, V.M., 1917. Construction and use of farm weirs. Farmers' Bulletin, 813, 1–18.

Cozzens, H.A., 1915. Flow over V-notch weirs. Power, 42, 21, 714.

Cuttle, S.P., Mason, D.J., 1988. A flow-proportional water sampler for use in conjunction with a V-notch weir in small catchment studies. Agr. Water Manage., 13, 93–99. https://doi.org/10.1016/0378-3774(88)90135-7

Eli, R.N., 1986. V-notch weir calibration using new parameters. J. Hydraul. Eng. - ASCE, 112, 4, 321–325. https://doi.org/10.1061/(ASCE)0733-9429(1986)112:4(321)

Ghodsian, M., 2004. Stage discharge relationships for triangular weir. Int. J. Civ. Eng., 2, 1, 1–7.

Greve, F.W., 1930. Calibration of 16 triangular weirs at Prude. Eng. News-Rec., 105, 5, 166–167.

Greve, F.W., 1932. Flow of water through circular, parabolic, and triangular vertical notch-weirs. Eng. Bulletin Purdue University, 40, 2–84.

Greve, F.W., 1945. Flow of liquids through vertical circular orifices and triangular weirs. Eng. Bull. Purdue University, 29, 3, 1–68.

Grossi, P., 1961. Su uno stramazzo triangolare in parete sottile, libero, con angolo al vertice molto piccolo (On a thin-plated, free triangular weir with a very small vertex angle). L'Acqua, 4, 99–100. (In Italian.)

Hattab, M.H., Mijic, A.M., Vernon, D., 2019. Optimised triangular weir design for assessing the full-scale performance of green infrastructure. Water, 4, 11, 773–790. https://doi.org/10.3390/w11040773

Hertzler, R.A., 1938. Determination of a formula for the 120-deg V-notch weir. Civil. Eng., 8, 11, 756–757.

Chanson, H., Wang, H., 2012. Unsteady discharge calibration of a large V-notch weir: REPORT No. CH88/12. 1. The University of Queensland, Brisbane, 282355720.

Chanson, H., Wang, H., 2013. Unsteady discharge calibration of a large V-notch weir. Flow Meas. Instrum., 29, 19–24. https://doi.org/10.1016/j.flowmeasinst.2012.10.010

ISO 1438, 2017. Hydrometry – Open channel flow measurement using thin-plate weirs. 3. ISO, Geneva.

Itaya, S., Takenaka, T., 1955. Measurement of oil flow by means of 60° sharp-edged triangular weir. Trans. Jpn. Soc. Mech. Eng., 21, 101, 94–96. (In Japanese.) https://doi.org/10.1299/kikai1938.21.94

JCGM 100, 2008. Evaluation of measurement data — Guide to the expression of uncertainty in measurement. 1. BIPM.

Ji, K., 2007. Discharge characteristics of V-shaped multi-slit weirs. Thesis. Concordia University, Montreal.

King, H.W., 1916. Flow of water over right-angled V-notch weir. The Michigan Technic, 29, 3, 189–195.

Lenz, A.T., 1942. Viscosity and surface tension effects on V-notch weir coefficients. Trans. Am. Soc. Civ. Eng., 351–374.

Martikno, R., Humaedi, M., Ashat, A., Situmorang, J., Novianto, Hadi, J., 2013. Evaluation of weirs calculation to estimate well capacity: a numerical study. In: Proc. 13th Indonesia International GEOTHERMAL Convention & Exhibition 2013. Jakarta. 332060750

Martínez, J., Reca, J., Morillas, M.T., López, J.G., 2005. Design and calibration of a compound sharp-crested weir. J. Hydraul. Eng. - ASCE., 131, 2, 112–116. https://doi.org/10.1061/(ASCE)0733-9429(2005)131:2(112)

Mawson, H., 1927. Applications of the principles of dimensional and dynamical similarity to the flow of liquids through orifices, notches and weirs. Proc. Inst. Mech. Eng., 112, 537–547.

Milburn, P., Burney, J., 1988. V-notch weir boxes for measurement of subsurface drainage system discharges. Can. Agr. Eng., 30, 2, 209–212.

Numachi, F., Hutizawa, S., 1941a. On the overflow coefficient of a right-angled triangular weir) (2. Notice). J. Soc. Mech. Eng., 44, 286, 286. (In Japanese.) https://doi.org/10.1299/jsmemag.44.286_5_1

Numachi, F., Hutizawa, S., 1941b. On the overflow coefficient of a right-angled triangular weir (2. Notice). Trans. Jpn. Soc. Mech. Eng., 7, 27–3, 5–9. (In Japanese.) https://doi.org/10.1299/kikai1938.7.27-3_5

Numachi, F., Hutizawa, S., 1942a. On the overflow coefficient of a right-angled triangular weir (3. Notice). J. Soc. Mech. Eng., 45, 308, 725. (In Japanese.) https://doi.org/10.1299/jsmemag.45.308_725_2

Numachi, F., Hutizawa, S., 1942b. On the overflow coefficient of a right-angled triangular weir (3. Notice). Trans. Jpn. Soc. Mech. Eng., 8, 33–3, 37–40. (In Japanese.) https://doi.org/10.1299/kikai1938.8.33-3_37

Numachi, F., Kurokawa, T., Hutizawa, S., 1940a. On the overflow coefficient of a right-angled triangular weir. J. Soc. Mech. Eng.,

43, 275, 45. (In Japanese.) https://doi.org/10.1299/jsmemag.43.275_45_2
Numachi, F., Kurokawa, T., Hutizawa, S., 1940b. On the overflow coefficient of a right-angled triangular weir). Trans. Jpn. Soc. Mech. Eng., 6, 22–3, 10–14. (In Japanese.) https://doi.org/10.1299/kikai1938.6.22-3_10
Numachi, F., Kurokawa, T., Tota, E., 1937. Influence of the surface of the weir edge of a right-angled triangular weir, which projected discontinuously upstream due to the creation of an overlap, on the flow coefficient. Trans. Am. Soc. Mech. Eng., 3, 11, 174–176. (In Japanese.) https://doi.org/10.1299/kikai1935.3.11_174
Numachi, F., Saito, I., 1948. On allowable shortest length of channel for triangular notch. J. Soc. Mech. Eng., 51, 357, 229–230. (In Japanese.) https://doi.org/10.1299/jsmemag.51.357_229_2
Numachi, F., Saito, I., 1951. On allowable shortest length of channel for triangular notch. Trans. Jpn. Soc. Mech. Eng., 17, 56, 1–3. (In Japanese.) https://doi.org/10.1299/kikai1938.17.1
O'Brien, M.P., 1927. Least error in V-notch weir measurements when angle is 90 degrees. Eng. News-Rec., 98, 25, 1030.
Piratheepan, M., Winston, N.E.F., Pathirana, K.P.P., 2007. Discharge measurements in open channels using compound sharp-crested weirs. J. Inst. Eng., 40, 3, 31–38. https://doi.org/10.4038/engineer.v40i3.7144
Pospíšilík, Š., 2020. 2.67° triangular-notch thin-plate weir. In: Juniorstav 2020. ECON Publishing, Brno, pp. 598–603. (In Czech.). https://juniorstav.fce.vutbr.cz/download
Pospíšilík, Š., 2021. Identification and quantification of uncertainties in the measurement and evaluation of the discharge coefficient of triangular-notch thin-plate weir. In: Juniorstav 2021. ECON Publishing, Brno, pp. 512–517. (In Czech.). https://juniorstav.fce.vutbr.cz/download
Pospíšilík, Š., 2022. Analysis of the exploration range of triangular–notch thin–plate weirs. In: Juniorstav 2022. 1. ECON Publishing, Brno, pp. 468–474. (In Czech.). https://juniorstav.fce.vutbr.cz/download
Pospíšilík, Š., Zachoval, Z., Pařílková, J., 2022. Characteristics of velocity field in short flume in front of triangular-notch thin-plate weir. In: Proc. 34th Symposium on Anemometry. Institute of Hydrodynamics CAS, Prague, pp. 40–49. (In Czech.)
Ramamurthy, A.S., Kai, J., Han, S.S., 2013. V-shaped multislit weirs. J. Irrig. Drain. Eng. - ASCE, 139, 7, 582–585. https://doi.org/10.1061/(ASCE)IR.1943-4774.0000574
Reddy, M.S., Reddy, Y.R., 2017. Experimental investigation on the influence of density of fluid on efficiency of V-notch. Int. J. Adv. Sci. Res. Eng., 3, 9, 35–41. https://doi.org/10.7324/%20IJASRE.2017.32515
Schlag, A., 1962. Note on flow measurement for triangular weir. La Tribune de Cebedeau. Liege, 15, 218, 22–24. (In French.)
Schoder, E.W., Turner, K. B., 1929. Precise weir measurements. Trans. Am. Soc. Civ. Eng., 1929, 93, 999–1190.
Shen, J., 1981. Discharge characteristics of triangular-notch thin-plate weirs: Studies of flow of water over weirs and dams. Geological survey water-supply paper, 1617-B. U. S. Government Printing Office, Washington.
Smith, E.S., 1934. The V-notch: Weir for hot water. American Society of Mechanical Engineers, 56, 9, 787–789.
Smith, E.S., 1935. The V-notch weir for hot water. Trans. Am. Soc. Mech. Eng., 57, 249–250.
Strickland, T.P., 1910. Mr. James Barr's experiments upon the flow of water over triangular notches. Engineering, 90, 598.
Switzer, F.G., 1915. Test of the effect of temperature on weir coefficients. Engineering News, 73, 13, 636–637.
Thomson, J., 1858. On experiments on the measurement of water by triangular notches in weir boards. In: Proc. Twenty-eight Meeting of the British Association for the Advancement of Science. John Murray, Albemarle street, London, pp. 181–185.
Thomson, J., 1861. On experiments on the gauging of water by triangular notches. In: Proc. Thirty-first Meeting of the British Association for the Advancement of Science. John Murray, Albemarle street, London, pp. 151–158.
Thornton, B.M., 1929. Measurement of fluid flow with triangular notches. Power Engineer, 24, 313–315.
Vatankhah, A.R., Khamisabadi, M., 2019. Stage-discharge relationship for triangular and curved-edge triangular weirs. Flow. Meas. Instrum., 69, 1–10. https://doi.org/10.1016/j.flowmeasinst.2019.101609
Vicena, D., 2020. Minimum head of triangular-notch thin-plate weir. Thesis. BUT, Brno. (In Czech.)
Viparelli, M., 1947. On the Thompson weir. In: Estratto da Atti Fondazione Politecnica del Mezzogiorno, 3, pp. 1–24. (In Italian.)
Wirak, L.R., 1934. An investigation of the flow of water over triangular weirs of different angles. Thesis. Princeton University, Princeton.
Yarnall, D.R., 1912. The V-notch weir method of measurement. J. Am. Soc. Mech. Eng., 34, 2, 1479–1494.
Yarnall, D.R., 1927. Accuracy of the V-notch-weir method of measurement. Trans. Am. Soc. Mech. Eng., 48, 939–964.

NOMENCLATURE

DN	diameter nominal
TPW	thin-plate weir
B	approach channel width [m]
C_d	discharge coefficient
$\bar{C}_d$	average discharge coefficient
g	standard acceleration due to gravity [m/s^2]
h	head [m]
h_e	effective head [m]
h_l	limit head [m]
h_{max}	maximum head [m]
h_s	minimum head of stable nappe [m]
k_h	height representing the combined effects of viscosity and surface tension [m]
P	weir height [m]
Q	discharge, measured discharge [m^3/s]
Q_C	computed discharge [m^3/s]
R^2	coefficient of determination
T	temperature [°C]
Z_b	bottom level [m]
Z_h	water surface level upstream in front of the weir at distance from $2h_{max}$ to $4h_{max}$ [m]
Z_P	crest level [m]
α	notch angle [°]
δQ	relative error of discharge

Received 3 October 2022
Accepted 13 December 2022